Orientation-enhanced growth and optical properties of ZnO nanowires grown on porous silicon substrates

Orientation-enhanced growth and optical properties of ZnO nanowires grown on porous silicon substrates

**Hsu-Cheng Hsu, Ching-Sheng Cheng, Chia-Chieh Chang,
Song Yang, Chen-Shiung Chang and Wen-Feng Hsieh**[1]

Department of Photonics and Institute of Electro-Optical Engineering, National Chiao Tung
University, 1001 Tahsueh Road, Hsinchu 30050, Taiwan

E-mail: wfhsieh@mail.nctu.edu.tw

Abstract
ZnO nanowires have been synthesized on porous silicon substrates with
different porosities via the vapour–liquid–solid method. The texture
coefficient analysed from the XRD spectra indicates that the nanowires are
more highly orientated on the appropriate porosity of porous silicon
substrate than on the smooth surface of silicon. The Raman spectrum
reveals the high quality of the ZnO nanowires. From the
temperature-dependent photoluminescence spectra, we deduced the
activation energies of free and bound excitons.

1. Introduction

One-dimensional (1D) materials have stimulated much
attention due to their promising potential in extensive
applications. The present research in this field focuses on
investigating the dependence of electrical transport, optical,
and mechanical properties on size and dimensionality [1, 2].
The semiconductor ZnO, which has a wide gap of 3.37 eV
and a large exciton binding energy of 60 meV, has been
recognized as a promising photonic material in the blue-
UV region. Due to their efficient excitonic emission and
self-formed cavity structure, ZnO nanowires on the *a*-plane
sapphire substrate have been demonstrated as the smallest laser
source [3]. Therefore, the ZnO nanowire has become one of the
most promising elemental building blocks in nanotechnology
applications [4–6].

Although vertically aligned ZnO nanorods on a sapphire
c-plane substrate via the hydride vapour-phase epitaxy
method have been reported [7], since sapphire is not
conductive and is relatively expensive, the application of
ZnO nanowires on sapphire in photonic devices is limited.
Therefore, ZnO nanowires grown on Si-based substrates
have received increasing interest for their low cost and

large size. The next-generation semiconductor nanowire-
based nanophotonic devices with the well-developed Si-based
technology will have many potential applications.

Unfortunately, the large mismatches in the thermal
expansion coefficients and the lattice constants would
introduce a rather large stress between the ZnO and the Si
substrate. This stress results in the growth of randomly
oriented ZnO nanowires. Many efforts [8–10] to prepare
ZnO nanowires on an Si substrate have not attained a
satisfactory quality due to the large stress. Recently, Fan
et al [11] reported self-oriented regular arrays of carbon
nanotubes by using a porous silicon substrate. Additionally,
porous silicon (PS) can emit red to blue emission with rather
easily obtainable red emitting in PS [12, 13]. A white
light source is achievable if the red emission from the PS
layers can be combined with the green emission from the
defect band of the ZnO and the blue-UV emission from the
ZnO excitonic emission. Herein we report an orientation
enhancement for ZnO nanowires with controlled-size porous
silicon substrates. Raman scattering characteristics for the
ZnO nanowire arrays were also studied. Photoluminescence
(PL) spectra are characterized by emissions from free and
donor-bound excitons. These exciton binding energies are also
determined by temperature-dependent PL spectra.

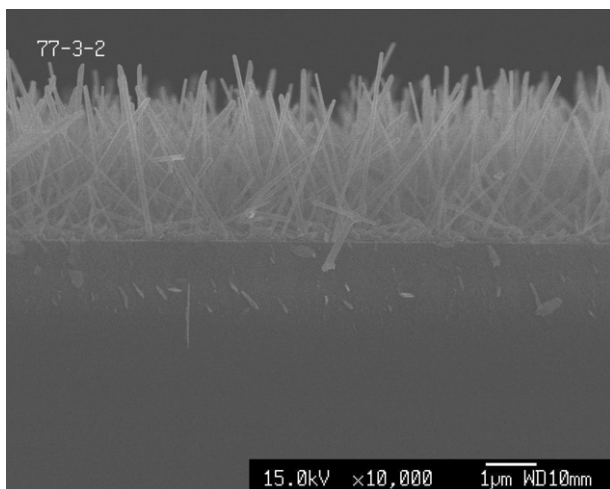[1] Author to whom any correspondence should be addressed.

Figure 1. SEM cross-sectional view image of the ZnO nanowires on PS.

Figure 2. TEM image showing the representative morphology of the ZnO nanowires. The inset shows the SAED patterns, revealing the monocrystalline phase nature of the nanowires.

2. Experiments

The porous silicon substrate was made by the electrochemical anodization method on (100) p+ Si substrates. Electrochemical etching was carried out for 2 min in a Teflon cell containing HF and ethanol with a 1:1 volume ratio with different current densities, between 10 and 80 mA cm^{-2}. Pt was used as a cathode. The resultant porous Si has a thin nanoporous layer. The porosity is a linear function of the current density for a specific HF concentration [16]. ZnO nanowires were synthesized by the vapour–liquid–solid (VLS) process [14], in which Au used as a catalyst was deposited on the porous silicon substrates by sputtering deposition. The Au-deposited porous Si substrates were placed on a quartz boat and then put into the centre of a quartz tube, 2.5 cm in diameter and 90 cm long, located in the middle of a high temperature cylindrical tube furnace. Two kinds of mixture of powders with ZnO and graphite (weight ratio 1:1) were used as the starting materials, and the furnace was mechanically pumped to a pressure of 5–30 Torr. The furnace temperature was increased to 950 °C at a rate of 50 °C min^{-1} and high-purity argon gas was then introduced to the quartz tube at a flow rate that ranged from 120 to 250 sccm. After the growth process was finished, the tube furnace was cooled slowly to room temperature in Ar-gas ambience. A white-violet coloured product was obtained on the surface of the Au-coated porous silicon. The structure and the alignment of the ZnO nanowires were characterized by x-ray diffraction (XRD) and with a scanning electron microscope (SEM). A 5 mW Ar-ion laser with an incident wavelength of 488 nm was used as the excitation source for the Raman spectroscopy. The scattered light was collected using backscattering geometry and detected by a SPEX 1877 Triplemate spectrometer equipped with a liquid nitrogen cooled CCD. The photoluminescence measurement was made using a 20 mW He–Cd laser at a wavelength of 325 nm and the emission light was dispersed by a TRIAX-320 spectrometer and detected by a UV-sensitive photomultiplier tube. A closed cycle refrigerator was used to set the temperature anywhere between 7 and 300 K.
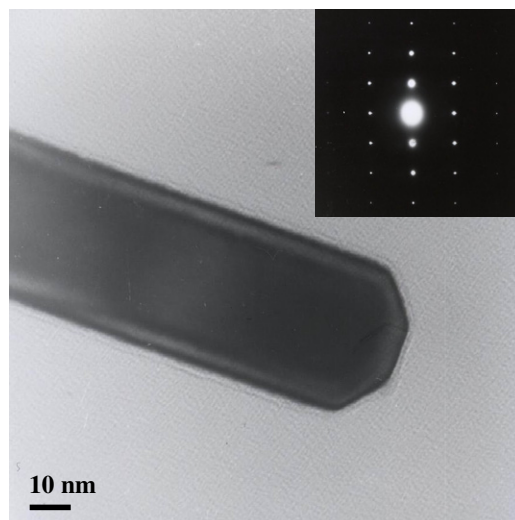
3. Results and discussion

A typical cross-sectional view SEM image of the high-density ZnO nanowires grown on a large area of the substrate is shown in figure 1. The majority of the nanowires are grown with a length of about 2–3 μm and diameters ranging from 20 to 200 nm. This micrograph reveals a high density of quasi-aligned nanowires uniformly distributed over the entire substrate. A TEM image (see figure 2) shows that the diameter of an individual ZnO nanowire is about 30 nm. The inset in figure 2 shows a typical selected area electron diffraction (SAED) pattern for a single ZnO nanowire. Along the same nanowire, the diffraction patterns are essentially identical, revealing that the nanowire is hexagonal wurtzite single-crystalline ZnO. The absence of even one droplet on the tip of a ZnO nanowire seems to imply that the growth mechanism is not followed by the VLS mechanism. This observation is due to the Au being infiltrated into the PS pores as the growth temperature is increased. The adhesive force between Au and PS was stronger than that between Au and plain Si. Therefore, Au as a catalyst stayed at the bottom of the nanowires when Zn vapour was introduced into the catalytic system. The above growth is still likely to be governed by the VLS mechanisms.

Figure 3(a) displays a typical XRD pattern for the ZnO nanowire. Major peaks were identified and compared with JCPDS file 36-1451, drawn at the bottom of the figure. This reveals that the product is composed of hexagonal ZnO with lattice constants $a = 0.325$ nm and $c = 0.522$ nm, which is in agreement with the JCPDS card for ZnO. Hence, these data from XRD and SAED analysis together further reveal that the ZnO nanowires are hexagonal wurtzite crystalline ZnO.

Furthermore, we used the texture coefficient (TC) [15] to determine the orientation of the ZnO nanowires. Normally, the growth direction of ZnO nanowires is [002] [3]. The TC can be expressed as the following expression:

$$TC_{(hkl)} = \frac{I_{(hkl)}/I_{0(hkl)}}{\frac{1}{N} \sum_N \left(\frac{I_{(hkl)}}{I_{0(hkl)}} \right)}, \qquad (1)$$
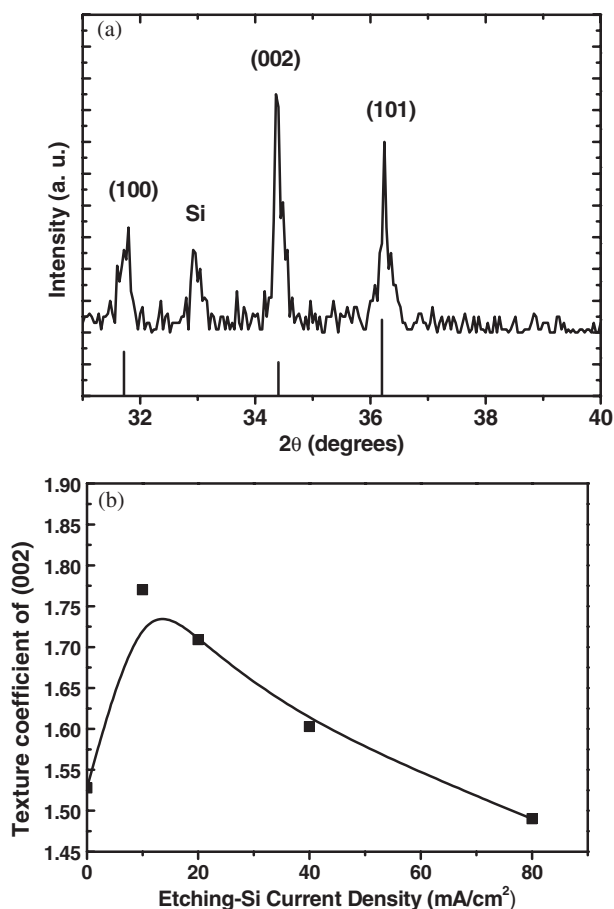
Figure 3. (a) Typical XRD spectra of the ZnO nanowires. (b) Texture coefficient of the ZnO nanowires as a function of the etching-Si current density.

where $I_{(hkl)}$ is the observed intensity of the (hkl) plane, $I_{0(hkl)}$ is the standard data (JCPDS 36-1451) of the (hkl) plane, and

N is the total number of diffraction peaks. When the TC value is larger than 1, a preferred orientation exists in the sample. We calculated three stronger diffraction peaks for ZnO nanowires, which are (100), (002) and (101). Figure 3(b) shows the TC of the (002) plane as a function of the current density of the etched silicon. Notably, the porosity increases with the etching current density for a specific HF concentration [16]. One can find that all of the TC values of the (002) plane are larger than 1, indicating the preferred orientation of the ZnO nanowires. The TC value (1.48–1.77) of ZnO nanowires grown on PS is larger than that of most other ZnO nanowires grown on silicon substrates [9, 10, 17], which are calculated and listed in table 1. The TC value of the ZnO nanowires grown on (110) sapphire [3], which is lattice matched with ZnO, is also listed in table 1 as a reference. The calculated TCs with different porosities for the porous silicon made by different current densities reveal that the porous silicon would benefit the growth orientation of ZnO nanowires. The possible reason for this is that the small current density makes the morphology of the silicon surface appear to have a ⟨111⟩ direction and helps ZnO nanowires grow in the ⟨002⟩ direction. With increasing current density, the morphology of porous silicon results in randomly directed growth of the ZnO nanowires, making the TC decrease.

To investigate the influence of the current density of the Si-etching on the diameter of nanowires, the diameters of the ZnO nanowires in all of the samples were carefully estimated from the SEM images. Figure 4 plots the histograms of the diameter distribution for ZnO nanowires grown on various substrates etched at different current densities. A Gaussian curve fitting to each of these histograms as solid curves yields a mean diameter of 83.5, 89.0, 72.4 and 60.0 nm for Si-etching densities under 10, 20, 40 and 80 mA cm^{-2}, respectively. Among these etching conditions, ZnO nanowires have the smallest mean size and the narrowest distribution on porous Si for the etching density of 80 mA cm^{-2}. This observation
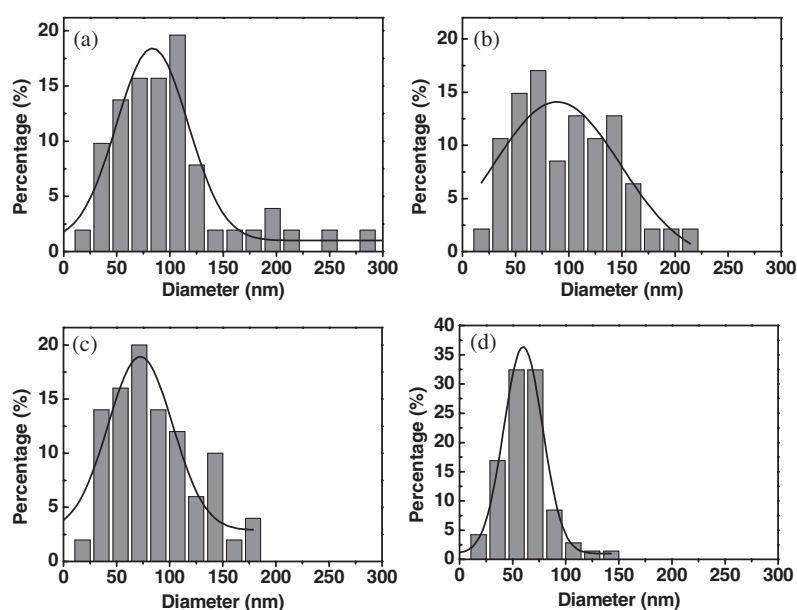

Figure 4. Histogram of the diameter of ZnO nanowires grown on porous Si for different etching current densities: (a) 10 mA cm^{-2} (b) 20 mA cm^{-2}; (c) 40 mA cm^{-2} and (d) 80 mA cm^{-2}.
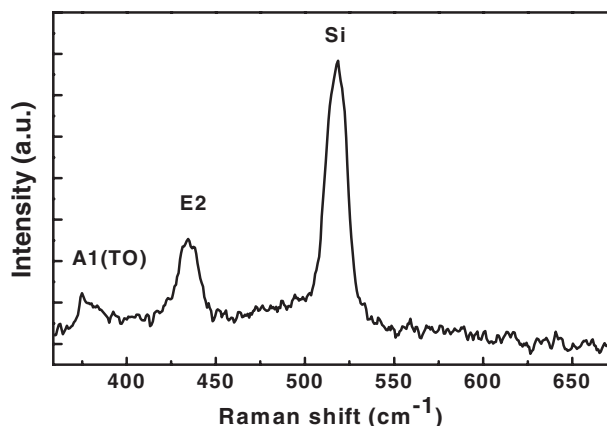
Figure 5. Typical Raman spectra of the ZnO nanowires.

Table 1. The calculated (002) texture coefficient value from previous works and this work.

TC value	Substrate	References
1.05	(100) Si	[9]
1.41	(100) Si	[10]
0.99	(100) Si	[17]
~3	(110) sapphire	[3]
1.48–1.77	Porous Si	This work

results from the monodispersity of the catalyst clusters on PS under the large etching current density. We have also grown the ZnO nanowires on Au-coated plain Si (100) substrates as a reference. The overall structures of the nanowires are similar to those grown on porous silicon. However, we found that the nanowires synthesized on plain silicon substrates have an even broader diameter distribution than those on PS substrates. Also, the nanowires appear to be less well aligned (lower TC $\sim$ 1.53) on plain silicon substrates than on the PS ones. Hence, we believe that these PS substrates would play an important role in controlling the orientated growth and narrowing the diameter distribution of ZnO nanowires.

According to group theory, wurtzite ZnO belongs to the space group C_{6v} with two formula units per primitive cell, and therefore the Raman-active phonon modes include E_2(low), E_2(high), A_1(LO), A_1(TO), E_1(LO), and E_1(TO). The only two B_1 modes are infrared and Raman inactive (silent modes) [18]. A typical Raman spectrum for ZnO nanowires grown on a silicon substrate is shown in figure 5. The observed phonon frequencies are A_1(TO) $\sim$ 380 cm^{-1} and E_2(high) $\sim$ 436 cm^{-1}. Since the penetration depth of the argon laser is longer than the length of the ZnO nanowires, a pronounced mode E_2(high) of the Si substrate at 520 cm^{-1} was also observed. The E_1(LO) is associated with a lattice defect, such as oxygen vacancies and zinc interstitial in the ZnO nanowires, which is similar to the previous results [19]. Clearly, this result with very weak E_1(LO) indicates that the sample is composed of ZnO with high quality hexagonal nanowires.

Figure 6(a) shows the PL spectra as a function of temperature. As the temperature is increased, the energy peaks shift to the low energy side due to the decrease of the band gap. The deconvolution of the low temperature (7 K) PL spectrum ranged from 3.34 to 3.39 eV by a series
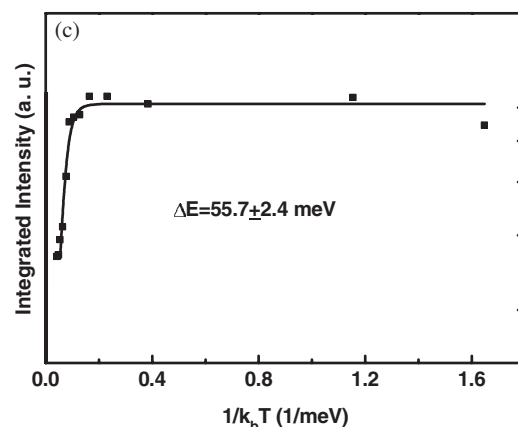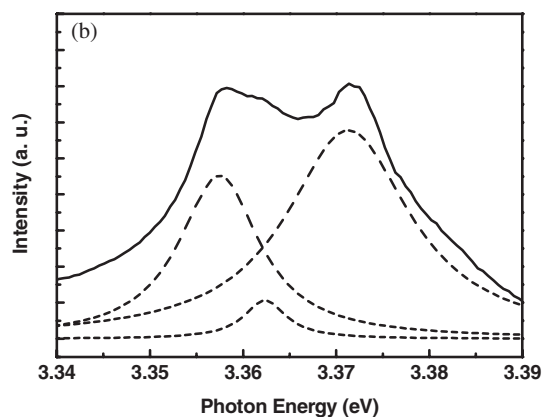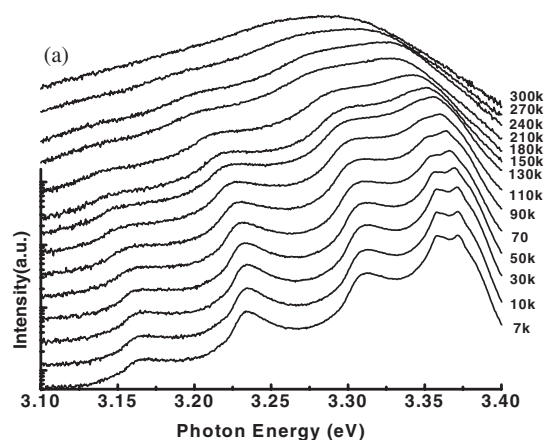

Figure 6. (a) PL spectra of ZnO nanowires in the temperature range 7–300 K. The intensities are plotted logarithmically. (b) The fitting results of PL measured at 7 K. (c) Integrated intensity of the free exciton of ZnO nanowires as a function of temperature with theoretical fitting curve.

of Lorentzian line profiles, as depicted in figure 6(b); the dominant luminescence lines at 3.358, 3.363, and 3.372 eV are assigned as two exciton-bound-to-defect emissions and a free exciton (FX) emission, respectively. On the lower energy side of the exciton peaks, the longitudinal optical (LO) mode of the FA at 3.31 eV and the peak at 3.24 eV are identified by the relative energy shift from the exciton peaks of higher order LO phonon replicas [20]. The strong exciton–phonon coupling in ZnO nanowires affects the FX-1LO phonon energy spacing because of the excitonic polaron formation. A further

increase in temperature causes the bound excitons localized by the defects to become free excitons, resulting in enhanced emission from the free excitons. Observably, the FX emission becomes the strongest when the temperature exceeds 30 K. As the temperature increases, the exciton linewidth is broadened due to scattering with LO phonons and the excitons become thermally ionized. The PL intensity exponentially decreases with increasing temperature due to the thermal ionization of the exciton and thermally activated nonradiative recombination mechanisms. Some of the bound excitons are thermally dissociated into free excitons, and the free excitons and their LO-phonon replicas dominate the PL spectrum. Finally, only free exciton emission and its one phonon replica can be observed at room temperature.

The dependence of the integrated PL intensity of the UV band on temperature is given in figure 6(c). The temperature dependence of the PL intensity can be expressed by the Arrhenius expression:

$$I(T) = \frac{I_0}{1 + A \exp\left(\frac{-\Delta E}{k_B T}\right)}, \qquad (2)$$

where ΔE is the activation energy of the thermal quenching process, k_B is the Boltzmann constant, I_0 is the emission intensity at 0 K, T is the thermodynamic temperature, and A is a constant. The result shows that the activation energy of about 55.7 meV is in agreement with the exciton binding energy of 60 meV for bulk ZnO crystal, which further supports our assessment that this emission band is from free exciton recombination.

In use of the Arrhenius-plot analysis, the activation energies of the two exciton-to-defect emissions were also obtained, corresponding to 8.8 and 13.6 meV. These values are in agreement with the binding energies of the exciton emission bound to neutral donors for the I_2 and I_4 emission lines, respectively [21, 22]. In addition, the exciton binding energies for the I_2 and I_4 lines estimated from their spectral positions are 9 and 14 meV, respectively, which agree well with the values calculated from temperature-dependent PL. These values are found to be exactly the same as the activation energy for thermal release of excitons from the neutral donors: $(D^\circ, X) \rightarrow D^\circ + X$.

4. Conclusions

We demonstrated the orientation enhancement of ZnO nanowires on PS by using a simple vapour deposition. The TC values from XRD spectra exhibit that the porous silicon substrate does benefit the orientation of growing nanowires. TEM and Raman measurements demonstrate that the ZnO nanowires have a high crystal quality. By fitting the PL spectra with the Arrhenius expression the activation energies of FXA and D°X were obtained. Synthesizing ZnO nanowires on a porous silicon substrate via the VLS method allows the growth of oriented nanowires.

Acknowledgments

References

[1] Gudiksen M S, Lauhon L J, Wang J, Smith D C and Lieber C M 2002 *Nature* **415** 617
[2] Huang Y, Duan X F, Cui Y, Lauhon L J, Kim K H and Lieber C M 2001 *Science* **294** 1313
[3] Huang M H, Mao S, Feick H, Yan H Q, Wu Y Y, Kind H, Weber E, Russo R and Yang P D 2001 *Science* **292** 1897
[4] Liu C H, Zapien J A, Yao Y, Meng X M, Lee C S, Fan S S, Lifshitz Y and Lee S T 2003 *Adv. Mater.* **15** 838
[5] Kind H, Yan H Q, Messer B, Law M and Yang P D 2002 *Adv. Mater.* **14** 158
[6] Hu P A, Liu Y Q, Fu L, Wang X B and Zhu D B 2004 *Appl. Phys.* A **78** 15
[7] Park W I, Kim D H, Jung S W and Yi G-C 2002 *Appl. Phys. Lett.* **80** 4232
[8] Dang H Y, Wang J and Fan S S 2003 *Nanotechnology* **14** 738
[9] Lee J S, Kang M I, Kim S, Lee M S and Lee Y K 2003 *J. Cryst. Growth* **249** 201
[10] Yuan H J *et al* 2003 *Chem. Phys. Lett.* **371** 337
[11] Fan S S, Chapline M G, Franklin N R, Tombler T W, Cassell A M and Dai H J 1999 *Science* **283** 512
[12] Canham L T 1990 *Appl. Phys. Lett.* **57** 1046
[13] Pavesi L 1997 *Riv. Nuovo Cimento* **20** 1
[14] Huang M H, Wu Y Y, Feick H, Tran N, Weber E and Yang P D 2001 *Adv. Mater.* **13** 113
[15] Lu J, Ye Z, Huang J, Wang L and Zhao B 2003 *Appl. Surf. Sci.* **207** 29
[16] Gaburro Z, Oton C J, Bettotti P, Dal Negro L, Prakash G V, Cazzanelli M and Pavesi L 2003 *J. Electrochem. Soc.* **150** C381
[17] Yang P, Yan H, Mao S, Russo R, Johnson J, Saykally R, Morris N, Pham J, He R and Choi H 2002 *Adv. Funct. Mater.* **12** 323
[18] Damen T C, Porto S P S and Tell B 1966 *Phys. Rev.* **142** 570
[19] Wu J J and Liu S C 2002 *J. Phys. Chem.* B **106** 9546
[20] Hsu H C and Hsieh W F 2004 *Solid State Commun.* **131** 371
[21] Heitz R, Fricke C, Hoffmann A and Broser I 1992 *Mater. Sci. Forum* **83** 1241
[22] Ko H J, Chen Y F, Yao T, Miyajima K, Yamamoto A and Goto T 2000 *Appl. Phys. Lett.* **77** 537